Ultrashort pulsed sinc-Gaussian light beams

Qing Cao

Institute of Electro-Optical Engineering, National Chiao Tung University, 1001 Ta Hsueh Road, Hsinchu, Taiwan 300, China, and Shanghai Institute of Optics and Fine Mechanics, Chinese Academy of Sciences, P.O. Box 800-211, Shanghai 201800, China

Sien Chi

Institute of Electro-Optical Engineering, National Chiao Tung University, 1001 Ta Hsueh Road, Hsinchu, Taiwan 300, China

Received October 26, 1999; revised manuscript received February 25, 2000

A family of analytical solutions of the time-dependent wave equation, the ultrashort pulsed sinc-Gaussian light beams (UPSGLB's), are presented in the paraxial approximation. Each of them has the product form of the monochromatic Gaussian light beam with the central frequency ν_c times the sinc function of the complex temporal–spatial beam parameter P_n. The complex temporal–spatial beam parameter P_n, which corresponds to the order n, is directly related to the temporal–spatial coupling properties of the nth-order UPSGLB. The UPSGLB's are used, for the first time to our knowledge, as an analytical expansion set for bandwidth-limited ultrashort light pulses emitted from mode-locked lasers with stable resonators (ULPEMLLSR's). Two special examples of bandwidth-limited ULPEMLLSR's, a single zeroth-order UPSGLB and a novel model of a nearly temporal–spatial Gaussian beam, are analytically investigated and compared with experimental results. [S0740-3224(00)02806-X]

OCIS codes: 320.0320, 270.5530, 140.4050, 050.1940.

1. INTRODUCTION

In the past several years the propagation and transformation of ultrashort light pulses have attracted much attention[1–24] because of the notable progress with the femtosecond laser technique.[25–28] Ziolkowski and Judkins[13] studied the temporal–spatial behaviors of the pulsed Gaussian beam whose initial field distribution is temporally spatially separable and revealed its temporal–spatial distortion properties. Recently, Wang *et al.*[14] introduced a new kind of pulsed Gaussian beam by taking into account the mode characteristics of mode-locked laser resonators and studied its temporal–spatial propagation behaviors. Unfortunately, Wang *et al.*'s pulsed Gaussian beam has the drawback that its transverse amplitude distribution grows boundlessly with the transverse coordinate r as $\exp(r^4)$ beyond a beamlike central region.[14,15] Based on Wang *et al.*'s work, Porras[15] introduced ultrashort pulsed Gaussian light beams by use of the analytic signals method and investigated their temporal–spatial propagation characteristics. On the other hand, by using the Fourier transform method, Heyman and Felsen[16] and Melamed and Felsen[17] also investigated ultrashort pulsed Gaussian light beams (in these two papers the ultrashort pulsed Gaussian light beams were more reasonably named isodiffracting pulsed beams because all the monochromatic Gaussian field components of these kinds of light beams have the same diffraction property). Especially, they analytically studied the example of analytic δ function pulsed beams.[16,17] More recently, Porras[18] and Cao[19] independently studied the subset of pulsed negative-power-function light beams. Feng and Winful[20] investigated the temporal–spatial transformation of isodiffracting pulsed beams by use of nondispersive quadratic phase media.

As a complete description for the ultrashort light pulses emitted from mode-locked lasers with stable resonators (ULPEMLLSR's), the fact that the real ULPEMLLSR's always have limited bandwidths should be taken into account, because the laser gain media used there, such as the Ti:sapphire media, always have limited net gain bandwidths. However, until now, only Eq. (25) of Ref. 15 has been concerned with the analytical solution to the problem of bandwidth-limited ULPEMLLSR's, and, in particular, no analytical expansion set for bandwidth-limited ULPEMLLSR's has been presented.

In this paper we shall analytically present a family of bandwidth-limited solutions of the time-dependent wave equation in the paraxial approximation and use them as an analytical expansion set for bandwidth-limited ULPEMLLSR's. The paper is organized as follows: In Section 2 we review the theoretical background for ULPEMLLSR's, which is very helpful for understanding the materials presented in this paper; in Section 3 we introduce the ultrashort pulsed sinc-Gaussian light beams (UPSGLB's) and investigate their temporal–spatial propagation characteristics; in Section 4 we develop a simple method to expand ULPEMLLSR's by UPSGLB's, give two special examples, and compare them with the real ultrashort light pulses observed by experiments; and in Section 5 we conclude this paper.

0740-3224/2000/071304-09$15.00

2. THEORETICAL BACKGROUND FOR ULPEMLLSR's

In free space a general polychromatic pulsed light beam is represented by a real function $V(x, y, t, z)$, which obeys the time-dependent wave equation

$$\left(\frac{\partial^2}{\partial x^2} + \frac{\partial^2}{\partial y^2}\right)V - \frac{1}{c^2}\frac{\partial^2 V}{\partial t^2} + \frac{\partial^2 V}{\partial z^2} = 0, \tag{1}$$

where c is the light speed in free space.

Usually, it is convenient to use the so-called analytic signal $\phi(x, y, t, z)$ to describe the temporal–spatial propagation properties of a polychromatic pulsed light beam.[29] The analytic signal $\phi(x, y, t, z)$ is defined as[29]

$$\phi(x, y, t, z) = 2\int_0^\infty \varphi(x, y, \nu, z)\exp(-i2\pi\nu t)\mathrm{d}\nu, \tag{2}$$

where $\varphi(x, y, \nu, z)$ is the Fourier transform of the real optical-field distribution $V(x, y, t, z)$ in time only; namely,

$$\varphi(x, y, \nu, z) = \int_{-\infty}^\infty V(x, y, t, z)\exp(i2\pi\nu t)\mathrm{d}t. \tag{3}$$

From Eq. (2) one can find that the analytic signal $\phi(x, y, t, z)$ has no negative frequency component at all. This property is different from that of the corresponding real optical-field distribution $V(x, y, t, z)$. Similar to the real optical-field distribution $V(x, y, t, z)$, the analytic signal $\phi(x, y, t, z)$ also obeys the time-dependent wave equation of Eq. (1). The relation between the real optical-field distribution $V(x, y, t, z)$ and its analytic signal $\phi(x, y, t, z)$ is simply given by[29]

$$V(x, y, t, z) = \mathrm{Re}[\phi(x, y, t, z)]. \tag{4}$$

The monochromatic field component $\varphi(x, y, \nu, z)$ corresponding to the frequency ν obeys the Helmholtz wave equation

$$\nabla^2\varphi + k^2\varphi = 0, \tag{5}$$

where $k = 2\pi\nu/c$ is the corresponding wave number in free space. In the paraxial approximation, the slowly varying part $U(x, y, \nu, z)$ of the monochromatic field component $\varphi(x, y, \nu, z) = U(x, y, \nu, z)\exp(ikz)$ obeys the following paraxial wave equation:

$$i2k\frac{\partial U}{\partial z} + \left(\frac{\partial^2}{\partial x^2} + \frac{\partial^2}{\partial y^2}\right)U = 0. \tag{6}$$

Let us now consider a general ULPEMLLSR. From laser beam and resonator theory,[30,31] we know that a spherical resonator (in Fig. 1, for simplicity, we consider only two-element resonators) is stable when $0 < g_1g_2 < 1$ [see Eq. (8) of Ref. 30], where $g_1 = 1 - L/R_1$, $g_2 = 1 - L/R_2$, L is the resonator length, and R_1,R_2 are the curvature radii of the two spherical mirrors. For a stable spherical resonator, there exist many longitudinal eigen frequencies and transverse eigenmodes. In the paraxial approximation the transverse fundamental modes corresponding to different eigenfrequencies are always Gaussian beams, while the longitudinal eigenfrequencies ν_m corresponding to the transverse fundamental modes are given by $\nu_m/\nu_0 = m + 1 + \pi^{-1}\arccos(\sqrt{g_1g_2})$ [see Eq. (56) of Ref. 30], where m is the order of the eigenfrequency and $\nu_0 = c/2L$ is the eigenfrequency interval. According to resonator theory,[30] all the fundamental mode Gaussian fields $U(x, y, \nu_m, z)$ of a stable spherical resonator that correspond to different eigenfrequencies ν_m have the same beam waist plane [its location is explicitly given by Eq. (55) of Ref. 30] and satisfy the simple relation that $\pi^2W_0^2(\nu_m)\nu_m = \mathrm{const}$ [see Eq. (54) of Ref. 30], where $W_0(\nu_m)$ is the waist width of the Gaussian field with the eigenfrequency ν_m. We shall for convenience choose the common waist plane as the $z = 0$ plane and use b to express the constant $\pi^2W_0^2(\nu)\nu$. According to Eq. (54) of Ref. 30, the parameter b can be determined to be

$$b = \pi c\left[\frac{L(R_1 - L)(R_2 - L)(R_1 + R_2 - L)}{(R_1 + R_2 - 2L)^2}\right]^{1/2}. \tag{7}$$

On the other hand, from mode-locked laser theory we know that, in an appropriate transverse-mode-selection arrangement, the total temporal–spatial optical field $\phi(x, y, t, z)$ of an ULPEMLLSR can be regarded as a linear superposition of the fundamental mode Gaussian fields with different eigenfrequencies ν_m and that the slowly varying parts $U(x, y, \nu_m, 0)$ of the monochromatic optical-field components $\varphi(x, y, \nu_m, 0)$ at the $z = 0$ plane can be expressed as[14,15,30,31]

$$U(x, y, \nu_m, 0) = g_m\frac{\pi}{b}\exp\left(-\frac{\pi^2r^2\nu_m}{b}\right), \tag{8}$$

where g_m expresses the weighting factor of the monochromatic Gaussian field with the eigenfrequency ν_m. From Eq. (8), the propagation law of paraxial Gaussian beams and the relation $\varphi(x, y, \nu_m, z) = U(x, y, \nu_m, z)\exp(ikz)$, one can obtain[30,31]

$$\varphi(x, y, \nu_m, z) = g_m\frac{\pi}{b + i\pi zc}\exp\left(i2\pi\frac{z}{c}\nu_m\right) \times \exp\left(-\frac{\pi^2r^2\nu_m}{b + i\pi zc}\right). \tag{9}$$

In practical mode-locked lasers, the output light pulses always have limited bandwidths because the net gain bandwidths of the laser devices always have limited distributions. As an important consequence, the orders m of the longitudinal eigenfrequencies should have a low limit m_1 and a high limit m_2. By taking these properties into account, the total temporal–spatial optical-field distribution $\phi(x, y, t, z)$ of an ULPEMLLSR can be expressed as

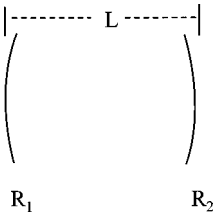

Fig. 1. Stable spherical resonator.

$$\phi(x, y, t, z) = 2 \sum_{m=m_1}^{m_2} \varphi(x, y, \nu_m, z) \exp(-i2\pi\nu_m t), \tag{10}$$

where $\varphi(x, y, \nu_m, z)$ is given by Eq. (9). As a good approximation, the discrete eigenfrequencies ν_m can be dealt with as a continuous variable ν, because, for an ULPEMLLSR, the eigenfrequency interval ν_0 is far smaller than the bandwidth $\Delta\nu$. For example, for a typical ultrashort light pulse emitted from a mode-locked Ti: sapphire laser, the eigenfrequency interval ν_0 is approximately of the order of 75 MHz (the corresponding resonator length L is 2 m), the bandwidth $\Delta\nu$ is approximately of the order of 100 THz (the corresponding wavelength range is 0.7–0.9 μm), and the ratio $\nu_0/\Delta\nu \approx 7.5 \times 10^{-7}$. In the above-mentioned approximation, the sum sign $\Sigma_{m=m_1}^{m_2}$ in Eq. (10) can be replaced by the integral sign $\int_{\nu_l}^{\nu_h} \mathrm{d}\nu$; namely, Eq. (10) can be approximately reexpressed as

$$\phi(x, y, t, z) = 2 \int_{\nu_l}^{\nu_h} \varphi(x, y, \nu, z) \exp(-i2\pi\nu t) \mathrm{d}\nu, \tag{11}$$

$$\varphi(x, y, \nu, z) = g(\nu) \frac{\pi}{b + i\pi zc} \exp\left(i2\pi \frac{z}{c}\nu\right) \times \exp\left(-\frac{\pi^2 r^2 \nu}{b + i\pi zc}\right), \tag{12}$$

where the discrete distribution function g_m (with the eigenfrequencies ν_m) has been replaced by its continuous envelope distribution $g(\nu)$. In Eq. (11) the values of the low-limit frequency ν_l and the high-limit frequency ν_h are given by $\nu_l = m_1\nu_0$ and $\nu_h = m_2\nu_0$, respectively. Equations (10) and (11) are both the solutions of the time-dependent wave equation of Eq. (1) in the paraxial approximation because the slowly varying parts of Eqs. (9) and (12) both satisfy the monochromatic paraxial wave equation of Eq. (6). The difference between Eq. (10) and Eq. (11) is that the former describes a train of ultrashort light pulses but the latter describes only one of them.[31] In the train of ultrashort light pulses, the pulses are separated from one another by a large time interval $2L/c$. Fortunately, in almost all cases, people are more interested in the temporal–spatial behavior of a single ultrashort light pulse than a pulse train. It is necessary to point out that, for an ideal ULPEMLLSR, all the monochromatic Gaussian field components $\varphi(x, y, \nu, z)$ have the same 0 phase at the $z = 0$ plane,[31] and therefore the weighting function $g(\nu)$ is a positive real function in this case.

From Eq. (12) one can find that, except for the constant factor πb^{-1}, the spectrum distribution $\varphi(0, 0, \nu, 0)$ of the on-axis near-field distribution $\phi(0, 0, t, 0)$ at the point ($r = 0$, $z = 0$) can be directly described by the weighting function $g(\nu)$. On the other hand, in most femtosecond laser experiments,[24–28] the measured spectrum distribution approximately equals the square of the weighting function $g(\nu)$, and the reconstructed pulsed intensity distribution from interferometric autocorrelation is approximately equal to the on-axis near-field intensity distribution $V^2(0, 0, t, 0)$ at the point ($r = 0$, $z = 0$). These properties will be very helpful for comparing our theoretical models with experimental results in Section 4.

3. ULTRASHORT PULSED SINC-GAUSSIAN LIGHT BEAMS

Let us now consider a family of special bandwidth-limited ULPEMLLSR's whose weight functions $g_n(\nu)$ have the form

$$g_n(\nu) = A_n \exp\left[i \frac{n\pi(\nu - \nu_c)}{\delta}\right] \tag{13}$$

in the range of $\nu_l \leqslant \nu \leqslant \nu_h$, where the orders n are integers; namely, $n = 0, \pm1, \pm2, \ldots$; $\nu_c = (\nu_h + \nu_l)/2$, is the central frequency; $\delta = (\nu_h - \nu_l)/2$, is the half-bandwidth; A_n is the normalization coefficient corresponding to the order n. We point out that the central frequency ν_c is different from the concept of the carrier frequency. The former is always valid for an arbitrary ultrashort light pulse with an arbitrary bandwidth, but the latter is meaningful only for the ultrashort light pulses that satisfy the quasi-monochromatic condition $(\nu_h - \nu_l) \ll (\nu_h + \nu_l)/2$. They are approximately equivalent only for quasi-monochromatic ultrashort light pulses.

Substituting Eq. (13) into Eqs. (12) and (11), one can obtain

$$\Phi_n(x, y, t, z) = -\frac{i2\pi\delta A_n}{(b + i\pi zc)P_n} \exp\left(-\frac{in\pi\nu_c}{\delta}\right) \times \left[\exp\left(\frac{iP_n\nu_h}{\delta}\right) - \exp\left(\frac{iP_n\nu_l}{\delta}\right)\right], \tag{14}$$

$$P_n = n\pi - 2\pi\delta\tau + \frac{i\delta\pi^2 r^2}{b + i\pi zc}, \tag{15}$$

where $\tau = t - z/c$ is the local time at the $z = z$ plane and P_n is the complex temporal–spatial beam parameter corresponding to the order n.

Equation (14) provides a family of analytical solutions of the time-dependent wave equation [Eq. (1)] in the paraxial approximation. These analytical solutions can be completely determined by four simple parameters δ, ν_c, (or ν_l, ν_h), b, and n. Note that the order n includes negative integer. From Eq. (14) one can deduce that none of these bandwidth-limited ultrashort light pulses has singularity because $\phi_n(x, y, t, z) \to 0$ when $\tau \to \pm\infty$ or when $r \to \infty$ or both.

In terms of the relations $\nu_h = \nu_c + \delta$, $\nu_l = \nu_c - \delta$, and $\exp(iu) = \cos(u) + i\sin(u)$, Eq. (14) can be reexpressed as

$$\phi_n(x, y, t, z) = \frac{4\pi\delta A_n}{b + i\pi zc} \exp(-i2\pi\nu_c\tau) \times \exp\left(-\frac{\pi^2 r^2 \nu_c}{b + i\pi zc}\right) \mathrm{sinc}(P_n), \tag{16}$$

where $\mathrm{sinc}(u) = \sin(u)/u$, is the sinc function. From Eq. (16) one can find that, except for the constant factor $4\pi\delta A_n$, each one of this family of bandwidth-limited ultrashort light pulses can be expressed as the product of the monochromatic Gaussian light beam $\exp(-i2\pi\nu_c\tau)$

$\times \exp[-\pi^2 r^2 \nu_c/(b + i\pi zc)]/(b + i\pi zc)$ with the central frequency ν_c times the sinc function of the complex temporal–spatial beam parameter P_n. For this reason, we name them ultrashot pulsed sinc-Gaussian light beams (UPSGLB's). Usually, the sinc function of the complex temporal–spatial beam parameter P_n can be regarded as the envelope of the nth-order UPSGLB when $\nu_c \gg \delta$, but note that this interpretation will become ambiguous and even meaningless when the central frequency ν_c becomes only a few times the half-bandwidth δ. Equation (16) also shows that the temporal–spatial coupling properties of the nth-order UPSGLB are completely determined by the complex temporal–spatial beam parameter P_n. Especially, as we show below, the real part of the parameter P_n directly describes the time delays with the increase of the coordinate variable r and with the increase of the order n.

We have a special interest in the temporal–spatial behaviors of UPSGLB's on the propagation axis. On the propagation axis the parameter P_n and the analytic signal $\phi_n(0,0,t,z)$ of the nth-order UPSGLB, respectively, reduce to $P_n = n\pi - 2\pi\delta\tau$ and

$$\phi_n(0,0,t,z) = \frac{4\pi\delta A_n}{b + i\pi zc}\exp(-i2\pi\nu_c\tau) \times \mathrm{sinc}(n\pi - 2\pi\delta\tau). \quad (17)$$

In particular, the on-axis near-field $\phi_n(0,0,t,0)$ and the on-axis far-field $\lim_{z\to\infty}\phi_n(0,0,t,z)$ further reduce to

$$\phi_n(0,0,t,0) = 4\pi\delta A_n b^{-1}\exp(-i2\pi\nu_c\tau) \times \mathrm{sinc}(n\pi - 2\pi\delta\tau), \quad (18)$$

$$\lim_{z\to\infty}\phi_n(0,0,t,z) = \frac{4\delta A_n}{zc}\exp(-i\pi/2)\exp(-i2\pi\nu_c\tau) \times \mathrm{sinc}(n\pi - 2\pi\delta\tau). \quad (19)$$

To our surprise, except for the factor b^{-1} in Eq. (18), the parameter b has no influence on the near-field and the far-field pulse profiles of UPSGLB's on the propagation axis. Equations (18) and (19) also reveal the interesting $-\pi/2$ Gouy phase shift between the on-axis near-field and the on-axis far-field. This property is very similar to that of the focused single-cycle electromagnetic pulse, which was pointed out by Feng *et al.*[23]

From laser beam and resonator theory[30,31] we know that the common complex spatial beam parameter q of the monochromatic eigen Gaussian fields $\varphi(x,y,\nu,z)$ of a stable resonator is given by

$$\frac{1}{q} = \frac{i\pi c}{b + i\pi zc}. \quad (20)$$

When this relation is substituted into Eq. (15), the complex temporal–spatial beam parameters P_n can be reexpressed as

$$P_n = -2\pi\delta\left(\tau - \frac{n}{2\delta} - \frac{r^2}{2cR}\right) + i\frac{\delta\pi r^2}{c}\mathrm{Im}\left(\frac{1}{q}\right), \quad (21)$$

where R is the real curvature radius and is given by $1/R = \mathrm{Re}(1/q)$. From Eq. (21) one can see that the real part of the complex temporal–spatial beam parameter P_n directly describes the time delays with the increase of the coordinate variable r and with the increase of the order n. Figure 2 provides the real optical-field distributions $V_n(0,0,t,0)$ of the negative first-order, the zeroth-order, and the positive first-order UPSGLB's at the point ($r = 0, z = 0$). The time delay of UPSGLB's with the increase of the order n is explicitly shown in Fig. 2. Figure 2 also shows that different UPSGLB's with different orders n give different emphasis on different time ranges. For example, the zeroth-order UPSGLB gives an emphasis on the time range that is near the $\tau = 0$ point. By the way, at the $z = 0$ plane, UPSGLB's have no time delay with the increase of the radial coordinate r because in this case the curvature radius R is infinite. Figure 3 shows the time delays of the zeroth-order UPSGLB with the increase of the coordinate r at the $z = 3.14\,m$ plane. In these two figures the parameters are chosen such that $\nu_l = 300\,\mathrm{THz}$ (the corresponding wavelength is 1.0 um), $\nu_h = 500\,\mathrm{THz}$ (the corresponding wavelength is 0.6 um), $\nu_c = 400\,\mathrm{THz}$, $\delta = 100\,\mathrm{THz}$, and $b = 3\pi^2 \times 10^8\,\mathrm{m^2\,s^{-1}}$.

By substituting the relations $z_R = b/(\pi c)$, $t' = \tau$, $\Delta t = 1/(\pi\delta)$, and $w_0 = 2\pi\nu_c$ into Eq. (25) of Ref. 15 and the expression $E = \varphi(x,y,z,t)\exp[iw_0(t - z/c)]$, one can prove that the example given by Eq. (25) of Ref. 15 is just the complex conjugate of the zeroth-order UPSGLB and therefore has the same real optical-field distribution $V(x,y,t,z)$ as the zeroth-order UPSGLB. This property shows that the example given by Eq. (25) of Ref. 15 is a special case of the UPSGLB's.

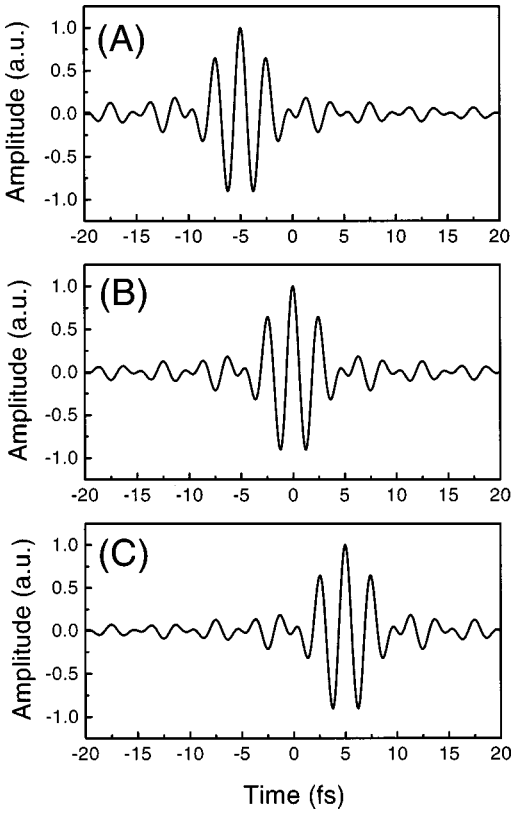

Fig. 2. Time delay with the increase of the order n at the point ($r = 0, z = 0$). (A) $n = -1$, (B) $n = 0$, and (C) $n = 1$. The parameters are chosen such that $\nu_c = 400\,\mathrm{THz}$, $\delta = 100\,\mathrm{THz}$, and $b = 3\pi^2 \times 10^8\,\mathrm{m^2\,s^{-1}}$.

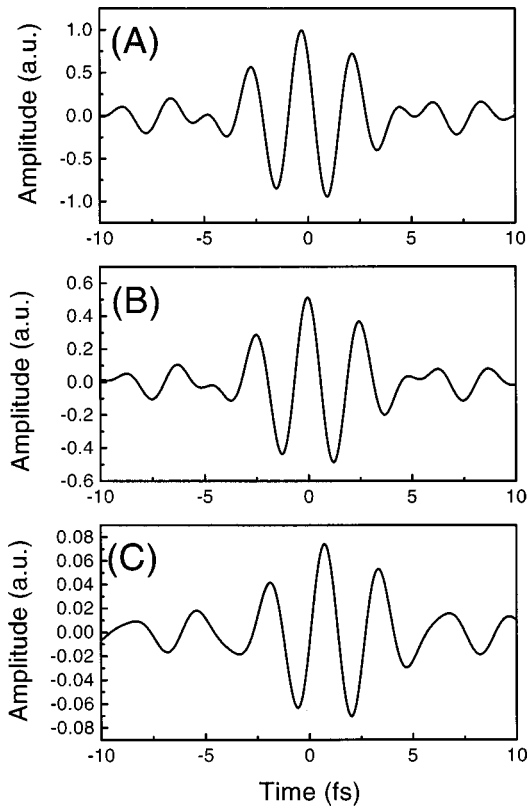

Fig. 3. Time delay with the increase of the radial coordinate r of the zeroth-order UPSGLB at the $z = 3.14\ m$ plane. (A) $r = 0.0$ mm, (B) $r = 1.0$ mm, and (C) $r = 2.0$ mm. The parameters are the same as in Fig. 2.

It is well known that the spectral density $D(\nu)$ of an ultrashort light pulse, which expresses the energy included in the monochromatic component $\varphi(x, y, \nu, z)$, is given by

$$D(\nu) = 2\int\int_{-\infty}^{\infty} |\varphi(x, y, \nu, z)|^2 \mathrm{d}x\,\mathrm{d}y. \tag{22}$$

The spectral density $D(\nu)$ is always independent of the longitudinal coordinate z because of the energy conservation law. Therefore one can conveniently evaluate the spectral density $D_n(\nu)$ of the nth-order UPSGLB at the $z = 0$ plane. Substituting Eqs. (13) and (12) into Eq. (22), the spectral density $D_n(\nu)$ of the nth-order UPSGLB can be determined to be

$$D_n(\nu) = \begin{cases} \pi {A_n}^2 b^{-1} \nu^{-1} & \text{for } \nu_l \leqslant \nu \leqslant \nu_h \\ 0, & \text{elsewhere} \end{cases}. \tag{23}$$

From Eq. (23) one can deduce that all UPSGLB's with different orders n have the same spectral density because $D_n(\nu)$ is independent of the orders n. This property is due to the fact that the quantities $g_n(\nu){g_n}^*(\nu)$ are independent of the order n. Equation (23) also shows that the spectral density $D_n(\nu)$ is equal to 0 in the ranges of $0 < \nu < \nu_l$ and of $\nu_h < \nu < \infty$. If we use wavelength $\lambda = c\nu^{-1}$ as the variable, the spectral density $D_n(\lambda)$ of the nth-order UPSGLB has a linear relation $D_n(\lambda) = \pi {A_n}^2 b^{-1} c^{-1} \lambda$ with wavelength λ in the range of $c\nu_h^{-1} \leqslant \lambda \leqslant c\nu_l^{-1}$. One can prove that this linear relation results from the property ${W_0}^2(\lambda) \propto \nu^{-1} \propto \lambda$. Substituting Eq. (23) into the normalization condition $E_n = \int_0^\infty D_n(\nu)\mathrm{d}\nu = 1$, the normalization coefficient A_n of the nth-order UPSGLB can be determined to be

$$A_n = \left\{ \frac{b}{\pi[\ln(\nu_h) - \ln(\nu_l)]} \right\}^{1/2}. \tag{24}$$

Equation (24) implies that all UPSGLB's with different orders n have the same normalization coefficient. Of course, this property is also due to the fact that the quantities $g_n(\nu){g_n}^*(\nu)$ are independent of the order n.

We know that, for a general polychromatic light beam, the instantaneous intensity $V^2(x, y, t, z)$ expresses the energy that flowed through the point (x, y, z) at the t moment.[29] However, for an ultrashort light pulse with an ultrawide bandwidth, the pulse duration is so short that the instantaneous intensity $V^2(x, y, t, z)$ is very difficult to measure. Fortunately, in this case, the time-integral intensity $I(x, y, z) = \int_{-\infty}^{\infty} V^2(x, y, t, z)\mathrm{d}t$ is still easy to measure. In fact, people usually use the time-integral intensity distribution $I(x, y, z)$ to describe the transverse properties of an ultrashort light pulse at the $z = z$ plane.[24,32,33] For example, under the intensity moment theory for polychromatic pulsed light beams, all the transverse intensity moments are defined on the basis of the time-integral intensity $I(x, y, z)$.[32,33] By the way, according to the intensity moment theory for polychromatic pulsed light beams, all the ULPEMLLSR's (including UPSGLB's) have the best beam quality because their monochromatic Gaussian field components satisfy the condition that ${W_0}^2(\nu)\nu = \text{const}$.[33]

In terms of Parseval's theorem, the relation $\varphi(x, y, -\nu, z) = \varphi^*(x, y, \nu, z)$, $|g_n(\nu)| = {A_n}^2$, and Eqs. (13) and (12), one can express the time-integral intensity $I_n(x, y, z)$ of the nth-order UPSGLB as

$$I_n(x, y, z) = \frac{2{A_n}^2\pi^2}{b^2 + \pi^2 z^2 c^2} \int_{\nu_l}^{\nu_h} \exp\left(-\frac{2\pi^2 b r^2 \nu}{b^2 + \pi^2 z^2 c^2} \right) \mathrm{d}\nu. \tag{25}$$

Simply integrating Eq. (25), one can further obtain

$$I_n(x, y, z) = \frac{2{A_n}^2}{br^2} \exp\left(-\frac{2\pi^2 b \nu_c r^2}{b^2 + \pi^2 z^2 c^2} \right) \times \sinh\left(\frac{2\pi^2 b\,\delta r^2}{b^2 + \pi^2 z^2 c^2} \right), \tag{26}$$

where $\sinh(u) = [\exp(u) - \exp(-u)]/2$ is the sinh function. From Eq. (26) one can find that all the UPSGLB's have the same time-integral intensity distribution because $I_n(x, y, z)$ is independent of the order n. In terms of the relation $\sinh(u) = \sum_{m=0}^{\infty} u^{2m+1}/(2m+1)! > u$ when $u > 0$, one can deduce that the time-integral intensity distribution $I_n(x, y, z)$ of the nth-order UPSGLB is always larger than the Gaussian intensity distribution

$$I(x, y, \nu_c, z) = \frac{4{A_n}^2\pi^2\delta}{b^2 + \pi^2 z^2 c^2} \exp\left(-\frac{2\pi^2 b \nu_c r^2}{b^2 + \pi^2 z^2 c^2} \right),$$

with the central frequency ν_c. On the other hand, from Eq. (25) one can deduce that the time-integral intensity $I_n(x, y, z)$ is always smaller than the Gaussian intensity distribution

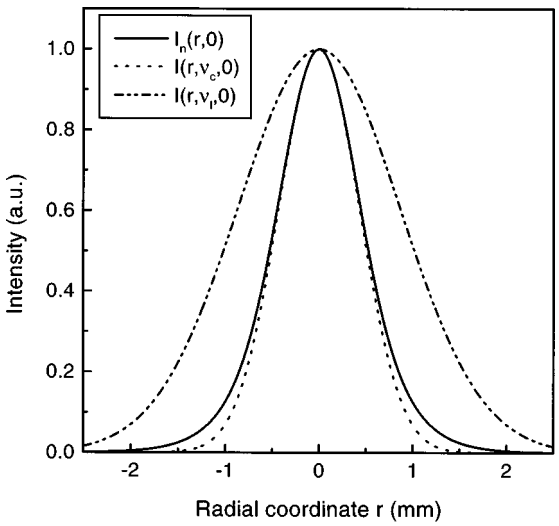

Fig. 4. Time-integral intensity distribution $I_n(r, 0)$ of a single UPSGLB at the $z = 0$ plane. The parameters are chosen such that $\nu_c = 400\,\mathrm{THz}$, $\delta = 300\,\mathrm{THZ}$, $z = 0$, and $b = 3\pi^2 \times 10^8\,\mathrm{m^2\,s^{-1}}$.

$$I(x, y, \nu_l, z) = \frac{4A_n{}^2\pi^2\delta}{b^2 + \pi^2 z^2 c^2}\exp\left(-\frac{2\pi^2 b\,\nu_l r^2}{b^2 + \pi^2 z^2 c^2}\right),$$

with the low-limit frequency ν_l. Therefore the time-integral intensity distribution $I_n(x, y, z)$ of the nth-order UPSGLB is always between the two Gaussian intensity distributions $I(x, y, \nu_c, z)$ and $I(x, y, \nu_l, z)$ at the $z = z$ plane. This property is explicitly shown in Fig. 4, where the parameters are chosen such that $\nu_c = 400\,\mathrm{THz}$, $\delta = 300\,\mathrm{THz}$, $b = 3\pi^2 \times 10^8\,\mathrm{m^2\,s^{-1}}$, and $z = 0$. From Fig. 4 one can find that the time-integral intensity distribution $I_n(x, y, z)$ of the nth-order UPSGLB at the $z = 0$ plane is a nearly Gaussian profile, but note that, strictly speaking, $I_n(x, y, z)$ is not a Gaussian distribution. It is worth mentioning that the time-integral intensity distribution $I_n(x, y, z)$ approaches the Gaussian intensity distribution $I(x, y, \nu_c, z)$ when $\delta \to 0$, because $I(x, y, \nu_l, z)$ also approaches $I(x, y, \nu_c, z)$ when $\delta \to 0$.

4. EXPANDING BANDWIDTH-LIMITED ULPEMLLSR's BY UPSGLB's

Let us now employ UPSGLB's to expand arbitrary bandwith-limited ULPEMLLSR's analytically. According to the Fourier series theory, in the range of $\nu_l \leqslant \nu \leqslant \nu_h$, an arbitrary weighting function $g(\nu)$ can be expanded as

$$g(\nu) = \sum_{n=-\infty}^{\infty} c_n A_n \exp\left[i\frac{n\pi(\nu - \nu_c)}{\delta}\right] = \sum_{-\infty}^{\infty} c_n g_n(\nu), \tag{27}$$

where the expansion coefficient c_n is given by

$$c_n = \frac{1}{2A_n\delta}\int_{\nu_l}^{\nu_h} g(\nu)\exp\left[-i\frac{n\pi(\nu - \nu_c)}{\delta}\right]\mathrm{d}\nu. \tag{28}$$

In particular, the expansion coefficient c_0 is simply given by $c_0 = \bar{g}(\nu)/A_n$, where $\bar{g}(\nu) = \int_{\nu_l}^{\nu_h} g(\nu)\mathrm{d}\nu/(2\delta)$ is the average of the weighting function $g(\nu)$ in the range of $\nu_l \leqslant \nu \leqslant \nu_h$. In terms of Eqs. (27), (12), and (11), the analytic signal $\phi(x, y, t, z)$ of the bandwidth-limited ULPEMLLSR with the above weighting function $g(\nu)$ can be finally expanded by

$$\phi(x, y, t, z) = \sum_{n=-\infty}^{\infty} c_n \phi_n(x, y, t, z), \tag{29}$$

where $\phi_n(x, y, t, z)$ is the nth-order UPSGLB, which is given by Eq. (16). Note that the expansion coefficients c_n are usually complex. As pointed out before, for an ideal ULPEMLLSR, its weighting function $g(\nu)$ is a positive real function. It can be proved that, in this ideal case, the expansion coefficients c_n have the property that $c_{-n} = c_n{}^*$. Therefore, for an ideal ULPEMLLSR, one can evaluate only the expansion coefficients of positive order UPSGLB's and then use the relation $c_{-n} = c_n{}^*$ to conveniently obtain the expansion coefficients of the corresponding negative order UPSGLB's. We emphasize that the expansion method developed in this section is generally valid because arbitrary weighting functions $g(\nu)$ can be strictly expanded by the Fourier series in the range of $\nu_l \leqslant \nu \leqslant \nu_h$. It is worth mentioning that the family of UPSGLB's are not orthogonal to one another (i.e., $\int\int\int_{-\infty}^{\infty}\phi_n(x, y, t, z)\,\phi_m{}^*(x, y, t, z)\mathrm{d}x\mathrm{d}y\mathrm{d}t \neq 0$ when $m \neq n$), although the Fourier series $g_n(\nu)$ are orthogonal to one another (i.e., $\int_{\nu_l}^{\nu_h} g_n(\nu)g_m{}^*\mathrm{d}\nu = 0$ when $m \neq n$) in the region of $\nu_l \leqslant \nu \leqslant \nu_h$.

To understand this expansion method better, let us now present two special examples.

Example 1: a single zeroth-order UPSGLB. As we pointed out before, for an ideal ULPEMLLSR, the weighting function is a positive real function. We find that the weighting function $g_0(\nu)$ of the zeroth-order UPSGLB is just a positive real function. This property implies that a single zeroth-order UPSGLB can be used to describe some real bandwidth-limited ULPEMLLSR's.

Figure 5 provides the on-axis near-field intensity distribution $V_0{}^2(0, 0, t, 0)$ of a zeroth-order UPSGLB at the point $(r = 0, z = 0)$. In Fig. 5 the parameters are chosen such that $\nu_l = 316\,\mathrm{THz}$ (the corresponding wavelength is

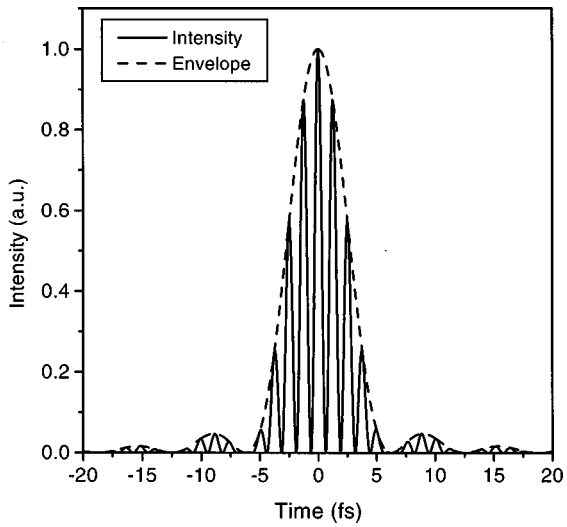

Fig. 5. Pulse intensity $V^2(0, 0, t, 0)$ of a single zeroth-order UPSGLB at the point $(r = 0, z = 0)$. The parameters are chosen such that $\nu_c = 396\,\mathrm{THz}$ and $\delta = 80\,\mathrm{THz}$.

~0.95 um), $\nu_h = 476\,\mathrm{THz}$ (the corresponding wavelength is ~0.63 um), $\nu_c = 396\,\mathrm{THz}$, and $\delta = 80\,\mathrm{THz}$. Comparing Fig. 5 with Fig. 4 of Ref. 28 [note that this figure is not the pulse intensity $V^2(0,0,t,0)$ but rather the interferometric autocorrelation of the real optical field $V(0,0,t,0)$] and with the inset of Fig. 1 of Ref. 27, one can find that the experimental results observed by Refs. 27 and 28 are very similar to the on-axis near-field intensity distribution ${V_0}^2(0,0,t,0)$ of the zeroth-order UPSGLB at the point $(r = 0, z = 0)$. These similarities show that the zeroth-order UPSGLB itself has practical meaning.

Example 2: a novel model of a nearly temporal–spatial Gaussian beam. The models of a nearly temporal–spatial Gaussian beam are very meaningful, because, in many practical cases, the ULPEMLLSR's indeed have such temporal–spatial behaviors.[24,26,31] Wang *et al.*[14] analytically investigated the temporal–spatial propagation problem of an ULPEMLLSR with a Gaussian weighting function. Unfortunately, they extended the integral region to the negative frequency domain and then made the solution diverge with larger r. To overcome this drawback, Porras[15] limited the integral region in the positive frequency domain and obtained a solution in terms of the error function with a complex variable [see Eq. (27) of Ref. 15]. However, Porras's treatment still has two drawbacks: One is that the solution is inconvenient to use because it is expressed as the complicated error function with a complex variable, and the other is that the weighting function used there is not bandwidth limited. To overcome these shortcomings, we now suggest a novel model of a nearly temporal–spatial Gaussian beam whose weighting function has the form

$$g(\nu) = 0.5A_n + 0.5A_n \cos[\pi(\nu - \nu_c)/\delta] \qquad (30)$$

in the range of $\nu_l \leqslant \nu \leqslant \nu_h$, where A_n is given by Eq. (24). Substituting this weighting function into Eq. (28), one can obtain $c_0 = 0.5$, $c_1 = c_{-1} = 0.25$, and $c_n = 0$ for other orders. Then the analytic signal $\phi(x,y,t,z)$ of the above-mentioned nearly temporal–spatial Gaussian beam can be expressed as

$$\phi(x,y,t,z) = 0.5\phi_0(x,y,t,z) + 0.25\phi_1(x,y,t,z) + 0.25\phi_{-1}(x,y,t,z). \qquad (31)$$

Figure 6 provides the weighting function $g(\nu)$, the near-field intensity distribution $V^2(0,0,t,0)$ at the point $(r = 0, z = 0)$, and the transverse intensity distribution $V^2(r,0,0)$ at the $z = 0$ plane at the original $t = 0$ moment. In this figure the parameters, for comparison with Ref. 26, are chosen such that $\nu_h = 375\,\mathrm{THz}$ (the corresponding wavelength is ~0.8 um), $\nu_l = 341\,\mathrm{THz}$ (the corresponding wavelength is ~0.88 um), $\nu_c = 358\,\mathrm{THz}$, $\delta = 17\,\mathrm{THz}$, and $b = 3.75\pi^2 \times 10^8\,\mathrm{m^2\,s^{-1}}$. Figure 6 explicitly shows the nearly temporal–spatial Gaussian intensity profile of the suggested model, which is very similar to many experimental results. In fact, Figs. 6(A) and 6(B) are very consistent with the experimental result of Ref. 26. Compared with the nearly temporal–spatial Gaussian beams introduced by previous papers,[14,15,31] our model has at least the following two advantages: One is that our model can be described by a simple analytical expression, and the other is that the weighting function $g(\nu)$ of our model is strictly bandwidth limited and therefore has more practical meaning.

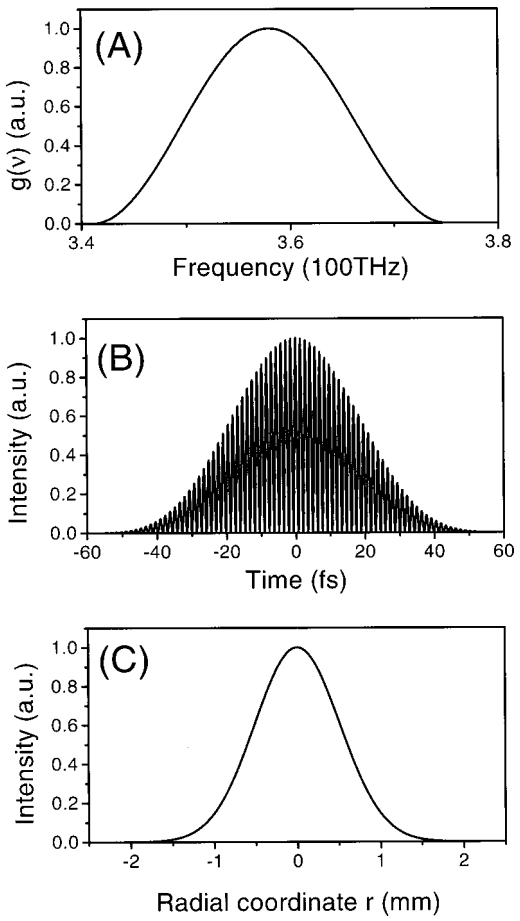

Fig. 6. Novel model of a nearly temporal–spatial Gaussian beam. (A) The weighting function $g(\nu)$, (B) the pulse intensity $V^2(0,0,t,0)$ at the point $(r = 0, z = 0)$, and (C) the transverse intensity distribution $V^2(r,0,0)$ at the $z = 0$ plane at the $t = 0$ moment. The parameters are chosen such that $\nu_c = 358\,\mathrm{THz}$, $\delta = 17\,\mathrm{THz}$, and $b = 3.75\pi^2 \times 10^8\,\mathrm{m^2\,s^{-1}}$.

5. CONCLUSIONS AND DISCUSSIONS

We have analytically presented a family of bandwidth-limited solutions of the time-dependent wave equation in the paraxial approximation. This family of solutions has the product forms of the monochromatic Gaussian light beam with the central frequency ν_c times the sinc function of the complex temporal–spatial beam parameter P_n and has been named ultrashort-pulsed sinc-Gaussian light beams (UPSGLB's). We have investigated their temporal–spatial evolution behaviors, and, in particular, we have revealed that the real part of the parameter P_n directly describes the time delays with the increase of the coordinate r and with the increase of the order n. As an important application, we have developed a simple method to expand bandwidth-limited ULPEMLLSR's by UPSGLB's analytically. To our knowledge, it is the first time that an analytical expansion set for bandwidth-limited ULPEMLLSR's is presented. In addition, we have analytically investigated two special examples of

bandwidth-limited ULPEMLLSR's, a single zeroth-order UPSGLB, and a novel model of a nearly temporal–spatial Gaussian beam and compared them with experimental results. The results obtained in this paper have practical meaning and can be used to study the temporal–spatial propagation problems of bandwidth-limited ULPEMLLSR's.

One may want to know whether these analytical UPSGLB's can be extended to the cases of linear propagation in dispersive media and nonlinear propagation (e.g., self-phase modulation and self-focusing) in Kerr media, because these propagation behaviors will definitely show up inside the laser resonators of femtosecond laser devices. Strictly speaking, the UPSGLB's cannot generally be extended to these two kinds of propagation behaviors. For the linear propagation in dispersive media, the simple propagation form [Eq. (12)] of the monochromatic Gaussian fields $\phi(x, y, \nu, z)$ corresponding to frequency ν becomes invalid, and, for the nonlinear propagation process in Kerr media (it is also the gain media at the same time), both the simple Fourier-type expansion and the simple propagation law of monochromatic Gaussian beam become invalid. Fortunately, as we discuss below, the UPSGLB's are still good models for describing the temporal–spatial propagation behaviors of ULPEMLLSR's, even if the dispersion, the self-phase modulation, and the self-focusing are all taken into account. Our analysis is as follows. (1) Except for the gain medium (i.e., the Ti:sapphire medium), all the other elements have only linear dispersion behaviors, which lead only to some phase differences among those monochromatic Gaussian fields $\varphi(x, y, \nu, z)$ when the total thickness of these elements is not too long. For simplicity, we consider only a dispersive medium with thickness D (the multiple dispersive elements can be treated similarly). After propagation through this dispersive medium, Eq. (12) should be added to a factor $\exp\{i2\pi[n(\nu) - 1]\nu D/c\}$, where the refractive index $n(\nu)$ describes the dispersive relation with the frequency ν. Apparently, this added factor can be included in the weighting function $g(\nu)$ of an ULPEMLLSR because it is independent of the radial coordinate r. (2) Approximately, the temporal propagation behaviors and the spatial propagation behaviors in the gain medium can be independently treated because the gain medium is very thin (usually the Ti:sapphire medium is only ~2.0-mm thick). (3) In the gain medium, the dispersion and self-phase modulation show a complicated solitonlike behavior and cannot be easily described by an analytical approach. Fortunately, we investigate only the output properties of an ULPEMLLSR in free space and do not investigate the complicated solitonlike behavior in detail. For the output behavior of an ULPEMLLSR, the dispersion and the self-phase modulation of the gain medium change only the weighting function $g(\nu)$, because the temporal and the spatial propagation behaviors in the gain medium can be independently treated. (4) As stated in items (1)–(3), the total influence of the dispersion and the self-phase modulation in a laser resonator is that they change the weighting function $g(\nu)$ of an ULPEMLLSR. In this paper we use only the family of UPSGLB's to expand an ULPEMLLSR analytically, and this expansion method is independent of the actual form of the weighting function $g(\nu)$. Therefore the dispersion and the self-phase modulation in a femtosecond laser resonator have no influence on the results of this paper. In addition, the change of the weighting function $g(\nu)$ resulting from the dispersion and the self-phase modulation has been compensated very well in femtosecond laser devices (especially in those sub-10-fs laser devices). Otherwise, no sub-10-fs light pulse can be obtained. (5) As a good approximation, the self-focusing effect in the gain medium can be treated as a lens[34–36] [i.e., the added phase is an approximate parabolic function of the radial coordinate r; see, for example, Eq. (4.1) of Ref. 34 or Eq. (3) of Ref. 36] when the light power is less than the critical power of self-trapping, because the transverse intensity distribution is a nearly Gaussian distribution and the gain medium is very thin [which ensures that the power-series approximation of Eq. (4.1) of Ref. 34 is valid]. According to the propagation law of Gaussian beams through a first-order optical system and the equivalent resonator theory,[37,38] this self-focusing lens changes only the actual values of the parameters b and z [which changes the longitudinal position of the common beam waist plane of the monochromatic Gaussian field distribution $\varphi(x, y, \nu, z)$] in Eq. (12) and does not change the expression form of Eq. (12) at all. That is to say, the output of an ULPEMLLSR is still an (approximate) isodiffracting pulsed beam even if the self-focusing lens in the gain medium is taken into account. Therefore the self-focusing effect in the thin gain medium has no influence on the results of this paper either.

ACKNOWLEDGMENTS

This research was partially supported by the National Science Council of China under contract NSC 88-2215-E-009-006. The authors are indebted to Thomas Elsaesser and the reviewers for their comments and proposals for improving the paper. The authors thank Ci-Ling Pan for some helpful discussions.

REFERENCES

1. M. Kempe, U. Stamm, B. Wilhelmi, and W. Rudolph, "Spatial and temporal transformation of femtosecond laser pulses by lenses and lens systems," J. Opt. Soc. Am. B **9**, 1158–1165 (1992).
2. Z. Bor and Z. L. Horváth, "Distortion of femtosecond pulses in lenses. Wave optical description," Opt. Commun. **94**, 249–258 (1992).
3. M. Kempe and W. Rudolph, "Femtosecond pulses in the focal region of lenses," Phys. Rev. A **48**, 4721–4729 (1993).
4. Z. L. Horváth and Z. Bor, "Focusing of femtosecond pulses having Gaussian spatial distribution," Opt. Commun. **100**, 6–12 (1993).
5. R. W. Ziolkowski and D. B. Davidson, "Designer pulsed beams for enhanced space–time focusing," Opt. Lett. **19**, 284–286 (1994).
6. A. S. Marathay, "Propagation of optical pulses with spatial and temporal dependence," Appl. Opt. **33**, 3139–3145 (1994).
7. E. Ibragimov, "Focusing of ultrashort laser pulses by the combination of diffractive and refractive elements," Appl. Opt. **34**, 7280–7285 (1995).
8. J. Paye and A. Migus, "Space–time Wigner functions and their application to the analysis of a pulse shaper," J. Opt. Soc. Am. B **12**, 1480–1490 (1995).
9. M. Gu and X. S. Gan, "Fresnel diffraction by circular and

serrated apertures illuminated with an ultrashort pulsed-laser beam," J. Opt. Soc. Am. A **13**, 771–778 (1996).
10. Z. Wang, Z. Xu, and Z. Zhang, "Diffraction integral formulas of the pulsed wave field in the temporal domain," Opt. Lett. **22**, 354–356 (1997).
11. J. M. Anderson and C. Roychoudhuri, "Diffraction of an extremely short optical pulse," J. Opt. Soc. Am. A **15**, 456–463 (1998).
12. I. P. Christov, "Propagation of femtosecond light pulses," Opt. Commun. **53**, 364–366 (1985).
13. R. W. Ziolkowski and J. B. Judkins, "Propagation characteristics of ultrawide-bandwidth pulsed Gaussian beams," J. Opt. Soc. Am. A **9**, 2021–2030 (1992).
14. Z. Wang, Z. Zhang, Z. Xu, and Q. Lin, "Space–time profiles of an ultrashort pulsed Gaussian beam," IEEE J. Quantum Electron. **33**, 566–573 (1997).
15. M. A. Porras, "Ultrashort pulsed Gaussian light beams," Phys. Rev. E **58**, 1086–1093 (1998).
16. E. Heyman and L. B. Felsen, "Complex-source pulsed-beam fields," J. Opt. Soc. Am. A **6**, 806–817 (1989).
17. T. Melamed and L. B. Felsen, "Pulsed-beam propagation in lossless dispersive media. I. Theory," J. Opt. Soc. Am. A **15**, 1268–1276 (1998).
18. M. A. Porras, "Nonsinusoidal few-cycle pulsed light beams in free space," J. Opt. Soc. Am. B **16**, 1468–1474 (1999).
19. Q. Cao, "Pulsed negative-power-function light beams," J. Opt. Soc. Am. B **16**, 1786–1789 (1999).
20. S. Feng and H. G. Winful, "Spatiotemporal transformation of isodiffracting ultrashort pulses by nondispersive quadratic phase media," J. Opt. Soc. Am. A **16**, 2500–2509 (1999).
21. R. W. Ziolkowski, "Localized transmission of electromagnetic energy," Phys. Rev. A **39**, 2005–2033 (1989).
22. R. W. Hellwarth and P. Nouchi, "Focused one-cycle electromagnetic pulses," Phys. Rev. E **54**, 889–895 (1996).
23. S. Feng, H. G. Winful, and R. W. Hellwarth, "Gouy shift and temporal reshaping of focused single-cycle electromagnetic pulses," Opt. Lett. **23**, 385–387 (1998).
24. L. Xu, G. Tempea, C. Spielmann, F. Krausz, A. Stingl, K. Ferencz, and S. Takano, "Continuous-wave mode-locked Ti: sapphire laser focusable to $5 \times 10^{13}\,\mathrm{W/cm^2}$," Opt. Lett. **23**, 789–791 (1998).
25. M. Nisoli, S. De Silvestri, O. Svelto, R. Szipöcs, K. Ferencz, C. Spielmann, S. Sartania, and F. Krausz, "Compression of high-energy laser pulses below 5 fs," Opt. Lett. **22**, 522–524 (1997).
26. I. P. Bilinsky, J. G. Fujimoto, J. N. Walpole, and L. J. Missaggia, "Semiconductor-doped-silica saturable-absorber films for solid-state laser mode locking," Opt. Lett. **23**, 1766–1768 (1998).
27. U. Morgner, F. X. Kärtner, S. H. Cho, Y. Chen, H. A. Haus, J. G. Fujimoto, E. P. Ippen, V. Scheuer, G. Angelow, and T. Tschudi, "Sub-two-cycle pulses from a Kerr-lens mode-locked Ti:sapphire laser," Opt. Lett. **24**, 411–413 (1999).
28. D. H. Sutter, G. Steinmeyer, L. Gallmann, N. Matuschek, F. M. Genoud, U. Keller, V. Scheuer, G. Angelow, and T. Tschudi, "Semiconductor saturable-absorber mirror-assisted Kerr-lens mode-locked Ti:sapphire laser producing pulses in the two-cycle regime," Opt. Lett. **24**, 631–633 (1999).
29. M. Born and E. Wolf, *Principles of Optics*, 5th ed. (Pergamon, Oxford, UK, 1975), pp. 494–499.
30. H. Kogelnik and T. Li, "Laser beams and resonators," Appl. Opt. **5**, 1550–1566 (1966).
31. W. Koechner, *Solid-State Laser Engineering*, 3rd ed. (Springer-Verlag, Berlin, 1992), pp. 482–485 and pp. 192–201.
32. P. M. Mejias and R. Martinez-Herrero, "Time-resolved spatial parametric characterization of pulsed light beams," Opt. Lett. **20**, 660–662 (1995).
33. Q. Cao and X. Deng, "Spatial parametric characterization of general polychromatic light beams," Opt. Commun. **142**, 135–145 (1997).
34. H. A. Haus, J. G. Fujimoto, and E. P. Ippen, "Analytic theory of additive pulse and Kerr lens mode locking," IEEE J. Quantum Electron. **28**, 2086–2096 (1992).
35. K. H. Lin and W. F. Hsieh, "Analytical design of symmetrical Kerr-lens mode-locking laser cavities," J. Opt. Soc. Am. B **11**, 737–741 (1994).
36. K. H. Lin, Y. Lai, and W. F. Hsieh, "Simple analytical method of cavity design for astigmatism-compensated Kerr-lens mode-locked ring lasers and its applications," J. Opt. Soc. Am. B **12**, 468–475 (1995).
37. H. Kogelnik, "Imaging of optical modes-resonators with internal lenses," Bell Syst. Tech. J. **43**, 455–494 (1965).
38. G. Herziger and H. Weber, "Equivalent optical resonators," Appl. Opt. **23**, 1450–1452 (1984).